Journal of Chromatography A, 1270 (2012) 246–253

Contents lists available at SciVerse ScienceDirect

Journal of Chromatography A

journal homepage: www.elsevier.com/locate/chroma

Discovery of candidate phospholipid biomarkers in human lipoproteins with coronary artery disease by flow field-flow fractionation and nanoflow liquid chromatography–tandem mass spectrometry

Seul Kee Byeon [a], Ju Yong Lee [a], Sangsoo Lim [a], Donghoon Choi [b], Myeong Hee Moon [a,*]

[a] Department of Chemistry, Yonsei University, Seoul 120-749, South Korea
[b] Cardiology Division, Cardiovascular Hospital, College of Medicine, Yonsei University, Seoul 120-752, South Korea

ARTICLE INFO

Article history:
Received 1 August 2012
Received in revised form 16 October 2012
Accepted 6 November 2012
Available online 12 November 2012

Keywords:
Lipoproteins
HDL
LDL
Phospholipid
Flow FFF
nLC–ESI-MS–MS

ABSTRACT

In this study, an analytical method is demonstrated to identify and develop potential phospholipid (PL) biomarkers of high density lipoprotein (HDL) and low density lipoprotein (LDL) in plasma from individuals with coronary artery disease (CAD) by employing a combination of off-line multiplexed hollow fiber flow field-flow fractionation (MxHF5) and nanoflow liquid chromatography–electrospray ionization-tandem mass spectrometry (nLC–ESI-MS–MS). HDL and LDL particles of human plasma were sorted by size at a semi-preparative scale using MxHF5, after which PL extracts of each lipoprotein fraction were qualitatively and quantitatively analyzed by nLC–ESI-MS–MS. Experiments were performed using plasma samples from 10 CAD patients and 10 controls. Quantitative analysis of the 93 PL species identified yielded a selection of 19 species from HDL fractions and 10 from LDL fractions exhibiting at least a five fold change in average concentration in CAD patients. Among the selected species, only a few were found exclusively in patient HDL fractions (18:3-LPA and 20:2/16:0-PG), control HDL fractions (16:0/16:1-PC, 20:1/20:4-PE, and 16:1-LPA), and control LDL fractions (16:0/22:3-PG). Moreover, 16:1/18:2-PC was detected from both HDL and LDL fractions of controls but disappeared in CAD patients. Although the typical change in lipoproteins for CAD is well known, with decreased levels of HDLs and reduced LDL particle size, the current study provides fundamental information on the molecular level of lipoprotein variation which can be utilized for diagnostic and therapeutic tracking.

1. Introduction

Phospholipids (PL) are types of lipids that constitute cell membranes in biological systems by forming a barrier called lipid bilayers. PLs have been shown to be responsible for various cellular responses such as cell growth, proliferation, and apoptosis [1,2], and many types of lipid metabolic disorders can manifest as human diseases [3,4]. Among different types of lipid species, PLs and lysophospholipids (LPLs) of which the latter classes share the same structure as PLs except that they have one acyl chain instead of two, have been revealed to play important roles in human diseases, and also as potential biomarkers [5]. Thus, analysis of PLs and LPLs from biological tissue and fluids (plasma or urine) is of interest, and several analytical methods have been developed with sophisticated usage of mass spectrometry (MS). Recent advances in MS have enhanced the capability of identifying lipid molecules with high resolution, sensitivity, and accuracy. Especially, electrospray ionization-MS (ESI-MS) with collision induced dissociation (CID), which forms protonated ions $[M+H]^+$ or deprotonated ions $[M-H]^-$ as well as charged adducts depending on a modifier, is commonly used for lipid investigation by two different approaches, namely, shotgun ESI-MS and chromatographic separation with ESI-MS. As opposed to the shotgun approach, where the sample is analyzed by a directional infusion method [6,7], liquid chromatography with MS (LC–ESI-MS–MS) can generate a more extensive library of lipid species based on composition because of its ability to detect low abundant lipid species. Indeed, this latter approach has been widely used to identify different types of lipids at the molecular level from various biological samples such as urine, plasma, serum, and cerebrospinal fluid [8–12].

As numerous types of treatments and medicines designed to treat diseases are currently being studied, disease biomarkers have become significant for various reasons, including early diagnosis and therapeutic purposes. Studies on discovering lipids as novel biomarkers of different types of diseases such as neurological disorders and cancers are systematically conducted in both chemical and clinical fields. In the literature, a number of studies have been performed using lipid analyses on human plasma or serum

* Corresponding author. Tel.: +82 2 2123 5634; fax: +82 2 364 7050.
E-mail address: mhmoon@yonsei.ac.kr (M.H. Moon).

0021-9673/$ – see front matter © 2012 Elsevier B.V. All rights reserved.
http://dx.doi.org/10.1016/j.chroma.2012.11.012

with ovarian and colorectal cancers to develop potential biomarkers [13–15]. Further, as one of the most common heart diseases throughout the world regardless of race and sex, coronary artery disease (CAD) is a major health risk and tends to manifest in people with a family history of CAD, low levels of high-density lipoprotein (HDL), high levels of low-density lipoprotein (LDL), high blood pressure, smoking habits, lack of exercise, and diabetes [16–20]. However, not many studies have dealt with lipids in different classes of lipoproteins such as HDL or LDL separately. Considering the fact that the extent of atherosclerosis is reportedly related to an elevated level of LDL and low level of HDL, which are known factors for developing various types of cardiovascular diseases, a comprehensive profiling of lipids from HDL and LDL separately is necessary to elucidate distinct traits of lipid patterns. For a quantitative and qualitative profiling of lipoprotein PLs, HDL and LDL particles need to be separated or isolated by a proper means prior to analysis. While density gradient ultracentrifuge (DGU) [21,22] and polyacrylamide gel electrophoresis (PAGE) [23,24] provide density based and size based fractionation, respectively, DGU requires a long operation time and PAGE requires an additional process to retrieve isolated lipoprotein particles from gels. Size exclusion chromatography (SEC) [25] performs well, however sample interaction with the stationary phase can be a possible risk leading to loss of the sample.

Flow field-flow fractionation (FlFFF) is an elution method to separate macromolecules, proteins, or protein complexes based on the difference in hydrodynamic diameters [26–28]. This method utilizes two different flow streams, namely, a migration flow along the FlFFF channel axis to elute sample components and a crossflow or radial flow acting perpendicular to the channel axis to retard sample migration, in a thin rectangular channel space of conventional FlFFF or in a cylindrical hollow fiber (HF) membrane of HF-FlFFF (or HF5). Separation in FlFFF is achieved in increasing order of hydrodynamic diameter of sample components since smaller particles or proteins, when driven by crossflow (or radial flow), extrude at a higher equilibrium position above the channel wall due to fast diffusion where the stream velocity of parabolic migration flow is higher than nearby the wall. FlFFF has been successfully utilized for size determination of HDLs and LDLs from human samples with various detection methods such as VIS detection using Sudan Black B (SBB) [29], multiangle light scattering (MALS) [30], online dual detection to determine cholesterol and triglycerides in serum lipoprotein [31], and fluorescence labeling [32]. Recently, multiplexed hollow fiber FlFFF (MxHF5), which consists of six individual hollow fiber (HF) channels connected together in parallel, was applied at a semi-preparative scale for size sorting of human lipoproteins, and it demonstrated that the phospholipids contained in HDL and LDL fractions can be profiled by nanoflow LC–ESI-MS–MS [10]. A notable difference between cylindrical MxHF5 and rectangular FlFFF channels is that the HF channel can be used as a disposable system and perform in single or multiple fashion. The disposable feature of HF channel reduces the carry-over effects and the possibility of multiple usage of HF increases sample throughput depending on the number of channels. An MxHF5 system can be easily assembled at low cost to speed up the process of collecting the fractionated HDL and LDL. Since there is no stationary phase in any FlFFF channel, it has a merit of dealing with nanometer-sized lipoproteins without the worry of sample interaction with stationary phase like in chromatography.

In this study, MxHF5 and nLC–ESI-MS–MS were employed for quantitative profiling of various phospholipids contained in both HDL and LDL particles in human plasma of patients with CAD and healthy controls. HDL and LDL fractions of plasma samples size-sorted by MxHF5 were collected from both 10 CAD patients and 10 healthy controls and the PL mixtures extracted from each fraction were analyzed by nLC–ESI-MS–MS. A total of 93 PL species including phosphatidylcholine (PC), phosphatidylethanolamine (PE), phosphatidylglycerol (PG), phosphatidylinositol (PI), phosphatidic acid (PA), and their lysophospholipid species were identified by data dependent collision induced dissociation (CID). PL species exhibiting a more than a five fold change in CAD patients relative to the concentration in controls were examined with principal component analysis (PCA) to develop potential biomarkers that can serve as a platform for understanding CAD in relation to the role of lipids in the human body.

2. Experimental

2.1. MxHF5 fractionation

Hollow fibers made up of polysulfone with a molar mass cut-off of 10 kDa (1.0 mm × 1.4 mm, I.D. × O.D.) were obtained from Wyatt Technology Europe GmbH (Dernbach, Germany) and were utilized for the assembly of the MxHF5. Fibers were cut out in a length of 25 cm, and each hollow fiber was inserted inside two equal pieces of glass tubing (1.8 mm × 3.5 mm × 10 cm), which were connected by a Teflon tee from Upchurch Scientific (Oak Harbor, WA, USA) at the center; 1/8 in. hand-tight ferrules and nuts were used to hold the glass tubes in place without distorting the fibers. At each end of the fibers extending out of the glass tubes, PEEK tubing (1.6 mm O.D. and 0.25 mm I.D.) was inserted inside the HF fiber with a length of 0.50 mm and tightened by 1/16 in. hand-tight ferrules and nuts along with Teflon unions from Upchurch. Six channels were assembled in an identical fashion and connected in parallel using a PEEK 7-port manifold at each end. A model SP930D solvent delivery pump (Young-Lin Instruments, Seoul, Korea) was used to deliver 0.1 M Tris-buffered saline (TBS), which was filtered with a 0.22 μm membrane filter prior to use, at a constant rate of 3.0 mL/min throughout the experiment. During the focusing/relaxation procedure, 1/10 of the pump flow was delivered through a capillary loop, a model 7125 loop injector (Rheodyne, Cotati, CA, USA), then onto channel inlets, while the remaining 9/10 of the flow traveled through the channel outlet, exiting through a radial flow only. The sample was injected to MxHF5 channels using this mode. After 3 min, the two converging flow streams were converted to the channel inlet only by switching the three-way and four-way valves, and then the flow exited the channel outlet at a rate of 0.8 mL/min (outflow rate) while the remaining 2.2 mL/min came out through the fiber walls of the six channels (radial flow rate).

Three protein standards, bovine serum albumin (BSA) (66 kDa), apoferritin (444 kDa), and thyroglobulin (670 kDa) were purchased from Sigma (St. Louis, MO, USA). Human plasma samples for ten healthy Korean individuals, consisted of four females and six males with age ranging from mid to late 20's, and four female and six male patients diagnosed with CAD and went under percutaneous coronary intervention, which is a procedure of inserting a deflated balloon in the clogged artery in order to widen the pathway so nearly normal blood flow can be achieved, in ages of early 30s to early 50s, were obtained from Severance Hospital (Seoul, Korea) under informed consent. Detection of proteins and HDL/LDL from plasma was made using a UV730D UV detector from Young-Lin Instrument (Seoul, Korea) at a wavelength of 280 nm for protein standards and 600 nm for HDL/LDL after staining. Prior to injection of plasma samples, 150 μL of human plasma was mixed with 15 μL of 1% SBB in dimethylsulfoxide, vortexed for 20 min, and then stored overnight at 4 °C to allow for complete staining. 50 μL of SBB stained plasma was injected to obtain a fractogram as shown in Fig. 1. With three consecutive injections, average peak areas of 3.37 ± 0.28 for HDL peaks and 1.37 ± 0.14 for LDL peaks were obtained, demonstrating consistent retention times for both peaks with reasonable

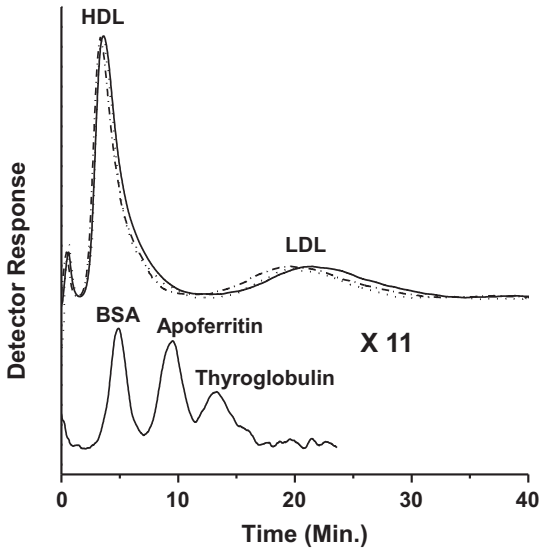

Fig. 1. Fractograms of MxHF5 separation of (a) HDL and LDL particles from 50 μL SBB stained human plasma detected at 600 nm and (b) three proteins standards (15 μg each) at 280 nm. Flow rate conditions for both runs was $\dot{V}_{out}/\dot{V}_{rad} = 0.8/2.2$ in mL/min.

standard deviations. However, for collecting HDL and LDL fractions of plasma, 50 μL of unstained plasma was injected at a time over two trials (total of 100 μL), the HDL and LDL fractions separated by MxHF5 were collected and concentrated to approximately 500 μL by centrifuging each fraction at 4000 × *g* for further experiments.

2.2. Extraction of PLs from collected HDL and LDL fractions

Lipid extraction using the modified Folch method with MTBE/methanol was used to remove proteins and extract LPLs and PLs simultaneously. [33] First, 200 μL of the HDL and LDL fractions was dried in a vacuum centrifuge for 3 h and 300 μL of methanol was added, quickly vortexed, and then placed in an ice water bath for 10 min. Next, 1000 μL of methyl-tert-butyl ether (MTBE) was added and vortexed for an hour for further incubation. After an hour, 250 μL of MS-grade water was added and mixed for 10 min. The sample was then centrifuged at 1000 × *g* for 10 min to form distinct aqueous and organic layers. The top organic layer was pipetted and transferred to a new vial, while 300 μL of methanol was added to the bottom aqueous layer and mixed for 10 min. The bottom layer was then sonicated with a tip for 2 min and centrifuged at 1000 × *g* for 5 min to collect the supernatant. The collected supernatant was combined with the previously saved top organic layer and dried in a vacuum centrifuge. The dried product was dissolved in $CHCl_3$:CH_3OH (1:1, v/v) and diluted with CH_3OH:CH_3CN (9:1, v/v) to a concentration of 160 μg/μL, and stored in a refrigerator for nLC–ESI-MS–MS analysis.

2.3. Profiling of PLs by nLC–ESI-MS–MS

An analytical column was prepared by pulling the tip of a 75 μm I.D./360 μL O.D. silica capillary tube from Polymicro Technology, LLC (Phoenix, AZ, USA) into a cone-shape by flame and packing it with a methanol slurry of 3 μm 100 Å Magic beads from Michrom Bioresources Inc. (Auburn, CA, USA). The column was cut into a length of 55 mm and connected to a 50 μm I.D. capillary tube that was extended from a 1200 capillary pump system from Agilent Technologies (Palo Alto, CA, USA) via a PEEK microcross. One of two other ends of the PEEK microcross was connected with a Pt wire for an electrical source, and the other with a capillary tube of 20 μm I.D. for vent flow. An on-off switch valve was deployed at the end of the vent capillary tube to switch the split and injection modes back and forth. A mobile phase solution composed of H_2O:CH_3CN (9:1, v/v) was used to load the sample onto the analytical column for 14 min at a flow rate of 0.5 μL/min and isopropanol/CH_3CN (9:1, v/v) was used to elute the sample at a total flow rate of 8 μL/min, while a continuous rate of 0.5 μL/min was allowed to pass through the analytical column with the rest of flow exiting through the vent capillary.

The composition for binary gradient nLC separation was 90/10 (v/v) dH_2O/CH_3CN for mobile phase A and 90/10 isopropanol/CH_3CN for mobile phase B. All organic solvents listed were of HPLC grade. In addition, 0.05% NH_4OH and 0.1% formic acid were used as modifiers to enhance ionization of PLs at negative and positive ion modes, respectively. In the positive ion mode, the gradient of mobile phase B was ramped to 60% over a minute and gradually increased to 100% over 30 min for separation, after which the column was washed with mobile phase B for another 20 min. In negative ion mode, mobile phase B was increased to 55% over a minute, increased to 60% over 14 min, 100% over the following 10 min, and then maintained at 100% for 25 min.

Prior to quantitative analysis of PL and LPL species from each HDL and LDL fraction, an LTQ Velos ion trap MS from Thermo Finnigan (San Jose, CA, USA) was utilized for nLC–ESI-MS–MS using data dependent CID experiments for structural identification. Eighty micrograms of lipid extracts from three control and three patient lipid extracts were injected in alternating turns for three times for the structural identification of LPLs and PLs. Next, 2.5 kV and 3.0 kV of voltage was applied for electrospray ionization (ESI) in positive and negative ion mode, respectively, and 40% of normalized collision energy was applied for collision induced dissociation (CID) in both ionization modes for PL analysis. Mass ranges of the precursor run for MS detection were 400–900 and 350–1000 amu for positive and negative ion modes, respectively. For CID experiments, a value of 2 for mass widths was applied in both modes. Identification of PL/LPL molecules was made from CID spectra obtained by nLC–ESI-MS–MS runs using LiPilot, an in-house software for the structural identification of phospholipids [34]. Quantitative analysis for identified PL and LPL species was carried out by using an LCQ Deca XP MAX ion trap from Thermo Finnigan for all ten control samples and ten CAD patient samples. In this case, only the precursor scan method was utilized for the identified PL and LPL species that were inserted to the data acquisition software as inclusion lists of detection. Next, the peak area of extracted chromatograms of each predetermined PL/LPL species was calculated. For the compensation of spectral fluctuation for each run, 300 fmol/μL of 13:0/13:0-phosphatidylcholine (PC) and 15:0/15:0-phosphatidylglycerol (PG), obtained from Avanti Polar Lipids Inc. (Alabaster, AL, USA), were added to each extract as internal standards for positive and negative ion mode, respectively. For each sample, triplicate nLC–ESI-MS runs were made for both positive and negative ion modes of MS. For PCA analysis, Minitab 15 software (http://www.minitab.co.kr) was utilized.

3. Results and discussion

Fig. 1 shows the fractograms of a healthy plasma sample (top) stained with SBB by MxHF5 showing the complete separation of HDL and LDL particles along with the separation of protein standards at the bottom. Since SBB slightly stains human serum albumin (HSA), the HDL peak may not reflect the intensity of stained HDL only. The MxHF5 fractograms of HDL/LDL were obtained by triplicate measurements to verify reproducibility. Since the injection volume of the stained plasma sample was 50 μL containing 45.5 μL of the original plasma sample, it demonstrated that semi-preparative separation of HDL and LDL could be achieved with the

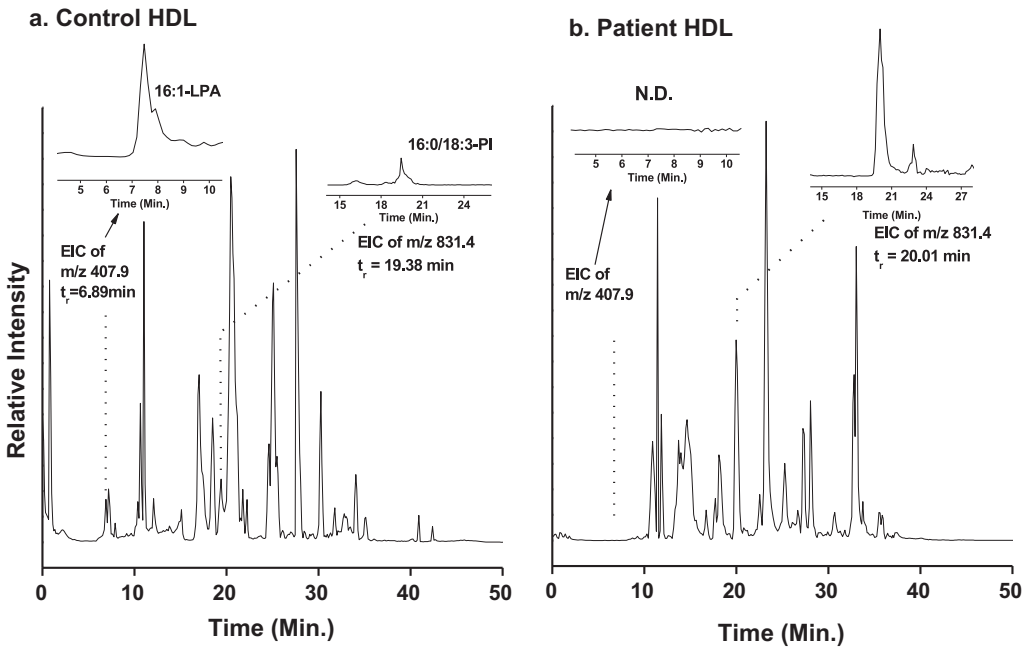

Fig. 2. Base peak chromatograms (BPCs) of (a) lipid extracts from the HDL fraction of a healthy control and (b) a patient plasma sample obtained by nLC–ESI-MS–MS along with extracted ion chromatograms (EICs) of *m*/*z* 407.9 and 831.4 as insets showing a significant change in peak area. Molecular structures of the two extracted ions were identified as 16:1-LPA and 16:0/18:3-PI, respectively.

current MxHF5 module having six HF fibers connected in parallel. For the collection of HDL and LDL fractions, 50 μL of unstained plasma sample was injected over two consecutive runs to accumulate each fraction. The collected HDL and LDL fractions not only contained lipids, but massive amount of proteins as well, thus the lipid extraction using MTBE/methanol was performed to remove proteins and extract as much lipid content as possible.

Fig. 2 illustrates the base peak chromatograms (BPCs) of lipid mixture samples extracted from each HDL fraction of (a) a control plasma and (b) a CAD patient plasma obtained by nLC–ESI-MS–MS at negative ion mode. In each BPC, extracted ion chromatograms (EICs) of two *m*/*z* values were inserted (explained below). During MS–MS experiments, PGs, PIs, PAs, LPAs, and LPGs were detected in negative ion mode, while PCs, PEs, LPCs, and LPEs were detected in positive mode. Structural identification of PL/LPL molecules was achieved by a precursor MS scan at each retention time slice followed by three sequential data dependent MS–MS scans. For example, based on the precursor MS scan shown in Fig. 3a obtained at a retention time of 19.38 min, which is marked with dotted line in Fig. 2a, CID experiments were carried out for the prominent precursor ion *m*/*z* 831.4 as shown in the CID spectra in Fig. 3b. The CID spectra shown in Fig. 3b represent the characteristic fragment ions such as typical loss of fatty acid from the precursor ion in the form of carboxylic acid as *m*/*z* 575.5 for $[M-H-R_1COOH]^-$ and 553.4 for $[M-H-R_2COOH]^-$. A similar pair of ions having *m*/*z* difference of 162 was observed at *m*/*z* 413.4 and 391.2, which represent the cleavage of fatty acid from the precursor ion without the inositol head group (162 Da) as $[M-H-162-R_1COOH]^-$ and for $[M-H-162-R_2COOH]^-$, respectively. Fragment ions showing the loss of fatty acid in the form of ketene were observed at *m*/*z* 593.6 and 409.4. In addition, cleaved carboxylate anions of acyl chains were found at *m*/*z* 255.5 and 277.9 for $[R_1COO]^-$ and $[R_2COO]^-$, respectively. Thus, the molecular structure of Fig. 3b was identified as 16:0/18:3-PI.

For quantitative analysis of PL molecules between control and patient samples, three control HDL and LDL samples and three CAD patient samples were thoroughly examined first to establish a list of PL/LPL molecules by using the nLC–ESI-MS–MS method as described above. From this global search, a total of 93 species (22 PCs, 9 LPCs, 7 PEs, 7 LPEs, 7 PAs, 7 LPAs, 12 PGs, 3 LPGs, and 19 PIs) were identified. The molecular structures of identified species are listed in Table S1 of supporting information, which contains the relative ratio of peak area of each species relative to that of the internal standard (IS). For quantitative analysis, only precursor MS scans without CID experiments were carried out for the identified PL and LPL species added as inclusion lists and the peak area of each target species was measured from extracted ion chromatograms (EICs). For the compensation of spectral fluctuation between nLC–ESI-MS runs, an internal standard (IS, 13:0/13:0-PC for positive and 15:0/15:0-PG for negative ion mode) was added to each lipid extract and the ratio of peak area relative to IS was reported.

Supplementary material related to this article found, in the online version, at http://dx.doi.org/10.1016/j.chroma.2012.11.012.

It is noteworthy that EICs of both 16:1-LPA (*m*/*z* 407.9) and 16:0/18:3-PI (*m*/*z* 831.4) in Fig. 2 showed a critical difference in the relative abundance between control and patient samples. The EIC in the left of Fig. 2a was extracted from *m*/*z* 407.9, of which the CID spectra yielded an identification of 16:1-LPA. While EIC of 16:1-LPA was detected from the control sample (relative peak area (vs. IS: 0.6 pmol of 15:0/15:0-PG) = 1.19 ± 0.33, $n = 10$), the same molecule was not detected from the HDL fraction of a CAD patient sample as shown with EIC in Fig. 2b. Interestingly, this species was not found in any of the ten patient HDL fractions, nor was it found in any of the LDL fractions from both patients and controls. A similar observation of significant up-regulation (greater than 7 fold) for patient samples was observed with 16:0/18:3-PI (12.00 ± 2.03 vs. 1.53 ± 0.39, $n = 10$ each) in the EICs of Fig. 2. However, the average up-regulation of the latter molecule in LDL fractions was less significant: 1.26 ± 0.24 (patients) vs. 0.61 ± 0.08 (controls) as listed in Table S1. In a biomarker study that involves multiple testing, use of Bonferroni correction of the significance level increases the stringency of the Student's *t*-test by lowering *p*-value that rejects the hypothesis, in an attempt to remove any false data [35]. With 95% confidence level and 93 detected lipid species, a newly corrected *p*-value (p') is 0.0005, obtained by using an equation, $p' = p/n$. Another statistical hypothesis test called Mann–Whitney

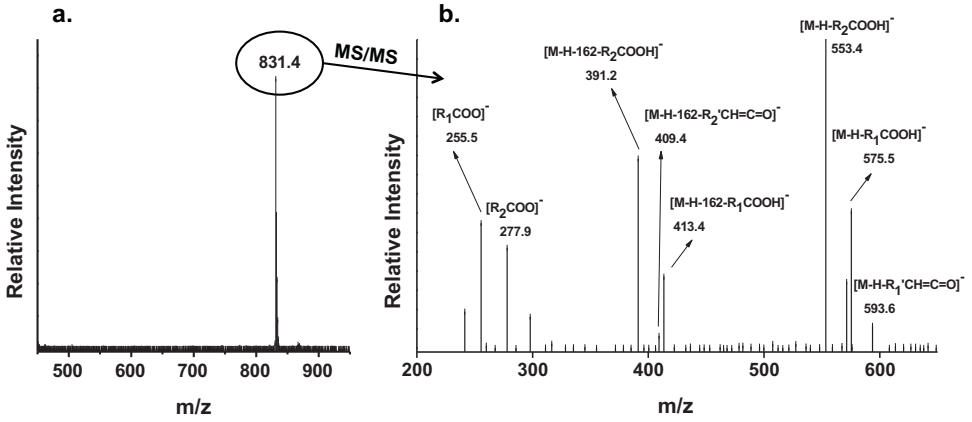

Fig. 3. MS spectra of (a) a precursor scan at t_r = 19.34 min of Fig. 2a and (b) data dependent CID experiment of the precursor ion m/z 831.4 showing the typical fragment ions used to identify its molecular structure as 16:0/18:3-PI.

test was applied to strengthen the discovery of candidate CAD markers. Among the lipids in Table S1 of Supporting Information, candidate biomarkers of CAD that exhibited significant differences according to p-values from t-test less than 0.0005 and those from Mann–Whitney test less than 0.05 with a greater than five fold difference between control and patient groups were selected. A total of 19 such species were identified (3 PCs, 2 LPCs, 1 PE, 1 LPEs, 1 PA, 5 LPAs, 4 PGs, 1 LPG, and 1 PIs) from the HDL fraction plotted in Fig. 4. Likewise, 10 candidate biomarker species (1 PC, 1 PE, 1 LPE, 1 PA, 3 PGs, and 3 PIs) were identified from the LDL fraction as shown in Fig. 5. Fig. 4 shows the plot of peak area ratio (peak area of target species vs. 0.6 pmol of IS) of selected PL and LPL species from HDL fractions: (a) up-regulated and (b) down-regulated species in patients. Among the 9 up-regulated species in Fig. 4a, 7 species that were not detected (marked as N.D. in the figure) in control HDL fractions were found in CAD patients. Moreover, concentrations of 16:0/18:3-PI were significantly increased in CAD patients, with some variation among

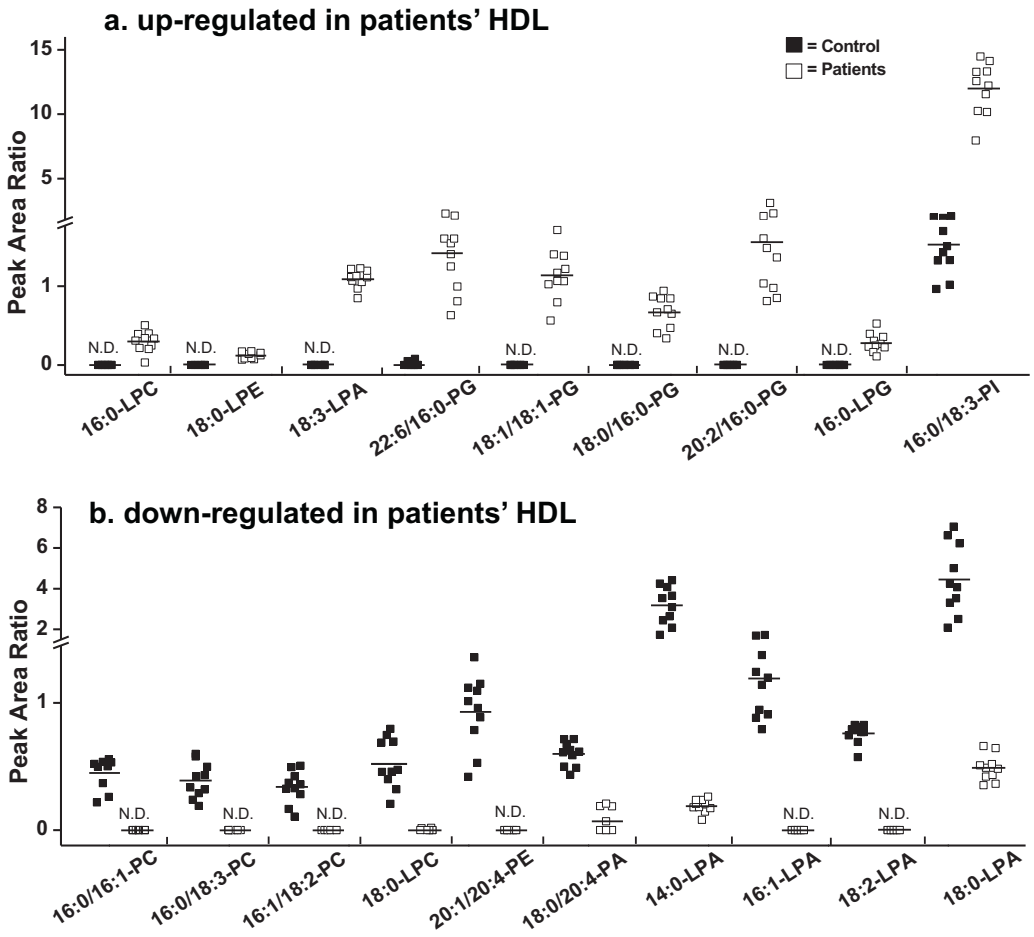

Fig. 4. Relative concentration of IS for selected PL and LPL species showing more than a 5-fold difference in patient HDL fractions compared to control HDL fractions: (a) up-regulated species and (b) down-regulated in patient HDL fractions (N.D. for not detected).

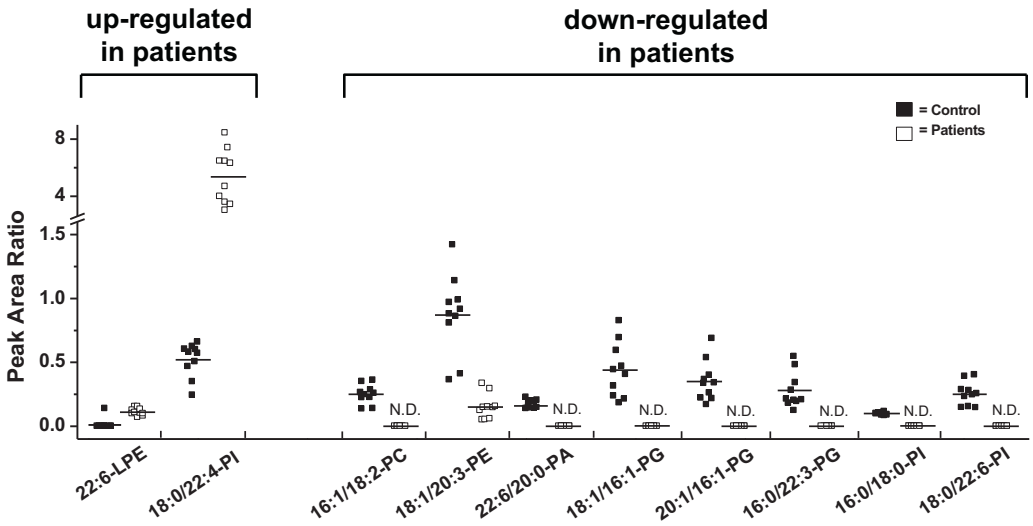

Fig. 5. Relative concentration to IS of selected species showing more than a 5-fold difference between patient and control LDL fractions.

controls. Among the selected down-regulated species in Fig. 4b, 6 out of 10 species were not detected at all in patient HDL fractions, with 14:0-LPA showing a significant decrease (16.7 fold) in patients while its concentration level in control samples was obviously high. For the LDL fractions in Fig. 5, most species (>5-fold of variation) were down regulated except 22:6-LPE and 18:0/22:4-PI, of which the latter showed a significant increase in patients. In addition, six species were not detected at all in patient samples. The relative peak areas and standard deviations of up- or down-regulated PL species that showed differences greater than five fold are listed in bold in Table 1.

As shown in Table 1, all PCs, LPCs, PE, PA, and LPAs that exhibited a greater than five fold difference (marked with bold) in both HDL and LDL fractions were down-regulated in patients except 16:0-LPC and 18:2-LPA. Conversely, all of the LPEs, PGs, LPG, and PIs (marked in bold in Table 1) that exhibited a greater than five fold difference were up-regulated in LDL fractions. For the examination of the different regulations between control and CAD patient sam-

Table 1
Candidate PL biomarkers of CAD from human lipoproteins showing a greater than five fold (marked in bold) difference in relative concentration between controls and patients. The relative concentration was determined as the ratio of average peak area of target species to that of internal standard. Candidate PL biomarkers were selected from the examined species in Table S1 of supporting information.

Class	PCA label	Molecular species	*m/z*	HDL		LDL	
				Control	Patients	Control	Patients
PC	C1	16:0/16:1	732.7	**0.50 ± 0.23**	**N.D.**	N.D.	N.D.
	C2	16:0/18:3	756.8	**0.39 ± 0.15**	**N.D.**	0.54 ± 0.07	0.65 ± 0.10
	C3	16:1/18:2	756.7	**0.34 ± 0.13**	**N.D.**	**0.25 ± 0.08**	**N.D.**
LPC	LC1	16:0	496.2	**N.D.**	**0.30 ± 0.13**	0.33 ± 0.49	0.32 ± 0.24
	LC2	18:0	524.4	**0.52 ± 0.20**	**0.00 ± 0.01**	N.D.	N.D.
PE	E1	18:1/20:3	768.7	0.41 ± 0.16	0.45 ± 0.32	**0.87 ± 0.35**	**0.15 ± 0.10**
	E2	20:1/20:4	794.5	**0.93 ± 0.29**	**N.D.**	N.D.	N.D.
LPE	LE1	22:6	526.4	0.80 ± 0.20	0.93 ± 0.31	**0.01 ± 0.04**	**0.11 ± 0.03**
	LE2	18:0	482.2	**N.D.**	**0.14 ± 0.07**	0.20 ± 0.16	0.25 ± 0.09
PA	A1	18:0/20:4	723.7	**0.60 ± 0.10**	**0.07 ± 0.09**	N.D.	N.D.
	A2	22:6/20:0	776.1	0.86 ± 0.22	0.41 ± 0.07	**0.16 ± 0.03**	**N.D.**
LPA	LA1	14:0	381.5	**3.19 ± 0.94**	**0.19 ± 0.05**	0.31 ± 0.06	0.66 ± 0.17
	LA2	16:1	407.9	**1.19 ± 0.33**	N.D.	N.D.	N.D.
	LA3	18:3	431.3	**N.D.**	**1.09 ± 0.12**	N.D.	N.D.
	LA4	18:2	433.3	**0.76 ± 0.08**	**N.D.**	0.38 ± 0.16	0.71 ± 0.25
	LA5	18:0	437.6	**4.46 ± 1.72**	**0.49 ± 0.10**	0.68 ± 0.28	0.49 ± 0.21
PG	G1	22:6/16:0	793.3	**0.00 ± 0.02**	**1.42 ± 0.53**	N.D.	N.D.
	G2	18:1/16:1	744.7	0.62 ± 0.15	1.17 ± 0.33	**0.44 ± 0.21**	**N.D.**
	G3	18:1/18:1	773.5	**N.D.**	**1.14 ± 0.32**	0.57 ± 0.15	0.61 ± 0.09
	G4	18:0/16:0	749.7	**N.D.**	**0.67 ± 0.21**	0.33 ± 0.11	0.11 ± 0.02
	G5	20:1/16:1	772.6	1.49 ± 0.68	0.59 ± 0.15	**0.35 ± 0.16**	**N.D.**
	G6	20:2/16:0	772.7	**N.D.**	**1.56 ± 0.74**	N.D.	N.D.
	G7	16:0/22:3	800.0	N.D.	N.D.	**0.28 ± 0.15**	**N.D.**
LPG	LG1	16:0	481.2	**N.D.**	**0.28 ± 0.12**	0.49 ± 0.13	0.52 ± 0.14
PI	I1	16:0/18:3	831.4	**1.53 ± 0.39**	**12.00 ± 2.03**	0.61 ± 0.08	1.26 ± 0.24
	I2	16:0/18:0	837.4	0.21 ± 0.06	0.22 ± 0.02	**0.10 ± 0.01**	**N.D.**
	I3	18:0/22:6	909.6	0.77 ± 0.19	0.82 ± 0.21	**0.25 ± 0.09**	**N.D.**
	I4	18:0/22:4	913.6	0.83 ± 0.38	4.25 ± 2.08	**0.52 ± 0.13**	**5.37 ± 1.78**

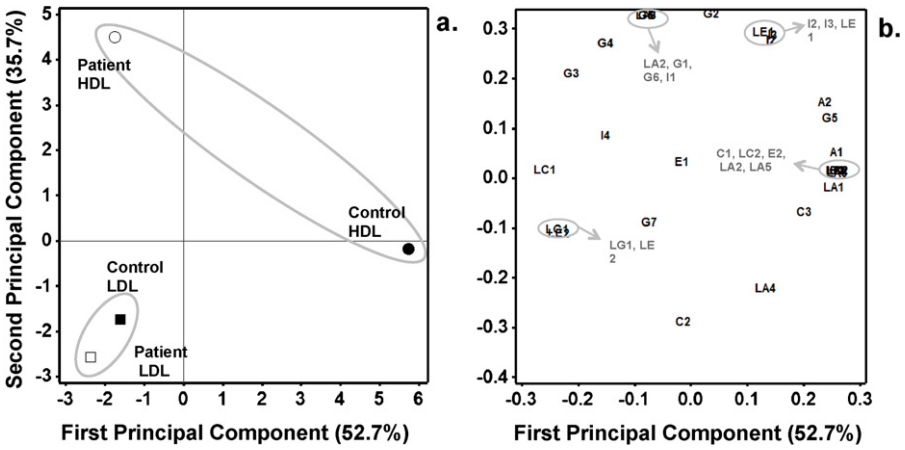

Fig. 6. PCA plots showing the statistical differences of PL and LPL species exhibiting a greater than 5-fold concentration difference between patient (open symbols) and control group (filled symbols) (left), and the distribution of individual components (right) of which labels of species match with the list in Table 1. The location of each species in the right plot represents the significant abundance of the sample group matching to the corresponding position of the left plot.

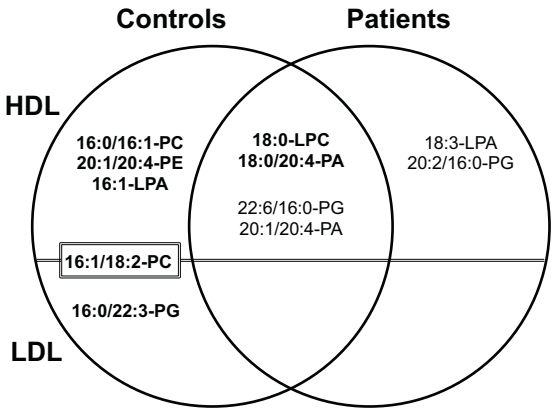

Fig. 7. Candidate PL and LPL biomarkers found exclusively in control (5 species in the left circle) and patient groups (two in the right circle). Molecules marked with bold in the overlapped region (center) represent the significant decrease (>5 fold) in patients while those with plain text denote a significant increase in patients.

ples, principal component analysis (PCA) was carried out for the PL species listed in Table 1 and plotted in Fig. 6. As seen in Table 1, evident clustering of the molecular species labeled as C1, LC3, E2, LA2, and LA5 in control HDL fractions than in patient HDL fractions are once again demonstrated in PCA plot, indicating that concentrations of these species are significantly reduced in CAD patients' HDL.

In Fig. 7, the PL species in Table 1 are classified in a diagram to sort out species detected from either controls or patients exclusively, or from both groups. For instance, 16:0/16:1-PC, 20:1/20:4-PE, and 16:1-LPA were found exclusively in control HDL fractions and disappeared in the patient group while 16:0/22:3-PG was found only in control LDL fractions. Conversely, 18:3-LPA and 20:2/16:0-PG were present in patient HDL fractions only. The species in the overlapped region of the two circles represent both controls and patients, with down-regulation in patients marked with bold (18:0-LPC, etc.) and up-regulation in patients in plain text. It was noted that 16:1/18:2-PC was unique species exhibiting in both HDL and LDL fractions of controls only and disappeared in the patient group.

4. Conclusions

By coupling MxHF5 and nLC–ESI-MS–MS, phospholipids in HDL and LDL particles in human blood were characterized qualitatively and quantitatively, and the combined method was applied to blood plasma samples from patients with CAD for the discovery of candidate biomarkers. While the well-known physical changes of lipoproteins of CAD patient consist of decreased HDL concentrations and decreased LDL particle sizes, this study reveals that there was a significant change in composition as well as concentration of phospholipids in each HDL and LDL fraction between control and CAD patient groups. From the quantitative analysis of identified PL/LPL species (26 LPLs and 67 PLs) in each HDL and LDL fraction of CAD patients, it was experimentally determined that some species were exclusively found or absent in patients plasma, meaning that those unique PL/LPL species can be utilized for the diagnostic or therapeutic traces of the development of CAD. Among them, 18:3-LPA and 20:2/16:0-PG may be potential indicators of CAD since they were found exclusively in patients' HDL fractions. Quantitative profiling of lipoproteic PLs can provide useful information for the study of metabolic pathways of PLs in relation to the status of cardiovascular disease. While the current study is focused on PLs and LPLs in relation to CAD, future work is necessary to elucidate the oxidized PLs/LPLs, since oxidation of lipoproteins is known to occur during the development of cardiovascular diseases.

Acknowledgements

This study was supported by a grant (No. 2011-0016438) from the National Research Foundation (NRF) of Korea funded by the Korean government (MEST).

References

[1] J.F. Brouwers, E.A. Vernooij, A.G. Tielens, L.M. van Golde, J. Lipid Res. 40 (1999) 164.
[2] M.M. Wright, A.G. Howe, V. Zaremberg, Biochem. Cell Biol. 82 (2004) 18.
[3] R. Meshkani, K. Adeli, Clin. Biochem. 42 (2009) 1331.
[4] L. Slama, C. Le Camus, L. Serfaty, G. Pialoux, J. Capeau, S. Gharakhanian, Diabetes Metab. 35 (2009) 1.
[5] C. Hu, R. van der Heijden, M. Wang, J. van der Greef, T. Hankemeier, G. Xu, J. Chromatogr. B 877 (2009) 2836.
[6] X. Han, R.W. Gross, J. Am. Chem. Soc. 118 (1996) 451.
[7] F.-F. Hsu, J. Turk, J. Chromatogr. B 877 (2009) 2673.
[8] R. Taguchi, T. Houjou, H. Nakanishi, T. Yamazaki, M. Ishida, M. Imagawa, T. Shimizu, J. Chromatogr. B 823 (2005) 26.
[9] S. Yu, Q. Li, T.M. Badger, N. Fang, Exp. Biol. Med. 234 (2009) 157.
[10] J.Y. Lee, H.K. Min, D. Choi, M.H. Moon, J. Chromatogr. A 1217 (2010) 1660.
[11] H.K. Min, G. Kong, M.H. Moon, Anal. Bioanal. Chem. 396 (2010) 1273.
[12] M. Kosicek, H. Zetterberg, N. Andreasen, J. Peter-Katalinic, S. Hecimovic, Neurosci. Lett. 516 (2012) 302.
[13] Y. Xu, Z. Shen, D.W. Wiper, M. Wu, R.E. Morton, P. Elson, A.W. Kennedy, J. Beilinson, J. Markman, G. Casey, J. Am. Med. Assoc. 280 (1998) 719.

[14] R. Sutphen, Y. Xu, G.D. Wilbanks, J. Fiorica, E.C. Grendys Jr., J.P. LaPolla, H. Arango, M.S. Hoffman, M. Martino, K. Wakeley, D. Griffin, R.W. Blanco, A.B. Cantor, Y.J. Xiao, J.P. Krischer, Cancer Epidemiol. Biomarkers Prev. 13 (2004) 1185.
[15] Z. Zhao, Y. Xiao, P. Elson, H. Tan, S.J. Plummer, M. Berk, P.P. Aung, I.C. Lavery, J.P. Achkar, L. Li, G. Casey, Y. Xu, J. Clin. Oncol. 25 (2007) 2696.
[16] J.K. Ninomiya, G. L'Italien, M.H. Criqui, J.L. Whyte, A. Gamst, R.S. Chen, Circulation 109 (2004) 42.
[17] J.O. Mudd, B.A. Borlaug, P.V. Johnston, B.G. Kral, R. Rouf, R.S. Blumenthal, P.O. Kwiterovich Jr., J. Am. Coll. Cardiol. 50 (2007) 1735.
[18] M. Roy, N. Mahmood, C. Rosendorff, Curr. Atheroscler. Rep. 12 (2010) 134.
[19] C.H. Mielke, J.P. Shields, L.D. Broemeling, Diabetes Res. Clin. Pract. 53 (2001) 55.
[20] L.W. Klein, N. Sandeep, J. Am. Coll. Cardiol. 41 (2003) 529.
[21] B.A. Griffin, M.J. Caslake, B. Yip, G.W. Tait, C.J. Packard, J. Shepherd, Atherosclerosis 831 (1990) 59.
[22] H.Y. Sun, S.F. Chen, M.D. Lai, T.T. Chang, T.L. Chen, P.Y. Li, D.B. Shieh, K.C. Young, Clin. Chim. Acta 411 (2010) 336.
[23] R.M. Krauss, D.J. Burke, J. Lipid Res. 23 (1982) 97.
[24] S.B. Alabakovska, B.B. Todorova, D.D. Labudovic, K.N. Tosheska, Clin. Chim. Acta 317 (2002) 119.
[25] P. Wiesner, K. Leidl, A. Boettcher, G. Schmitz, G. Liebisch, J. Lipid Res. 50 (2009) 574.
[26] J.C. Giddings, Science 260 (1993) 1456.
[27] K.G. Wahlund, J.C. Giddings, Anal. Chem. 59 (1987) 1332.
[28] P. Reschiglian, M.H. Moon, J. Proteom. 71 (2008) 265.
[29] I. Park, K.J. Paeng, Y. Yoon, J.H. Song, M.H. Moon, J. Chromatogr. B 780 (2002) 415.
[30] D.C. Rambaldi, A. Zattoni, S. Casolari, P. Reschiglian, D. Roessner, C. Johann, Clin. Chem. 53 (2007) 2026.
[31] D.C. Rambaldi, P. Reschiglian, A. Zattoni, D. Roessner, C. Johann, Anal. Chim. Acta 654 (2009) 64.
[32] J.Y. Ahn, K.H. Kim, J.Y. Lee, P.S. Williams, M.H. Moon, J. Chromatogr. A 1217 (2010) 3876.
[33] S.K. Byeon, J.Y. Lee, M.H. Moon, Analyst 137 (2012) 451.
[34] S. Lim, S.K. Byeon, J.Y. Lee, M.H. Moon, J. Mass Spectrom. 47 (2012) 1004–1014.
[35] D. Broadhurst, D.B. Kell, Metabolomics 2 (2007) 171.